*cyclo*Saligenyl-mannose-1-monophosphates as a New Strategy in CDG-Ia Therapy: Hydrolysis, Mechanistic Insights and Biological Activity

Ulrike Muus,[a] Christian Kranz,[b] Thorsten Marquardt,[b] and Chris Meier*[a]

Keywords: Glycosylation / *cyclo*Saligenyl-pyranose-1-phosphate / *cyclo*Sal / Drug design / CDG-**Ia**

Phosphomannomutase 2 (PMM-2) deficiency leads to an inefficient intracellular formation of mannose-1-phosphate (**1**), which causes an inherited metabolic disease with multisystemic abnormalities (*C*ongenital *D*isorder of *G*lycosylation type **Ia**, CDG-**Ia**). In order to circumvent this metabolic deficiency, the *cyclo*Sal approach was applied for the intracellular delivery of mannose-1-monophosphate (**1**). *cyclo*Saligenyl-pyranose-1-monophosphates **6**–**11** were obtained by a phosphitylation/oxidation procedure starting from appropriately protected D-pyranoses. The chemical hydrolysis data and the involved hydrolysis mechanisms of *cyclo*saligenyl-mannose-1-monophosphates **6**–**9** and their epimeric glucose analogues **10**, **11** are reported. Furthermore, the biological activity of *cyclo*Sal-mannose-1-phosphates **6**–**9** was tested in vitro in PMM-2-deficient fibroblasts. 3-Methyl-*cyclo*Sal-2,3,4,6-tetra-*O*-acetyl-α-D-mannopyranose-1-monophosphate (**8**) showed a total correction of the phenotype, thus proving the delivery of mannose-1-phosphate. This may offer a suitable possibility for a therapy of CDG-**Ia**.

Introduction

The congenital disorders of glycosylation syndrome (CDG) are autosomal recessively inherited disorders first described by J. Jaeken in 1980.[1,2] CDGs are classified into two types corresponding to the type and intracellular localization of the glycosylation pathways. CDG-**I** are disorders of the assembly of the lipid-linked oligosaccharide (LLO) at the membrane of the endoplasmic reticulum and the transfer of the oligosaccharide from the dolichol anchor to selected residues of nascent polypeptides. CDG-**II** involves disorders of the *N*-glycan processing occurring in the endoplasmic reticulum or the Golgi apparatus, or disorders affecting the assembly of *O*-glycans. Protein glycosylation plays an important role in the metabolism, function and structure of glycoconjugates.[3] Due to the hypoglycosylation of several proteins in CDG most patients suffer from liver insufficiency, growth retardation, cardiomyopathy, and often cerebral dysfunction and statomotor retardation.[4]

The most frequent CDG-type is CDG-**Ia**, with more than 500 patients known to date. The genetic defect is located in one of the early steps in the synthesis of *N*-linked glycans. This defect leads to a significant reduction in the concentration of phosphomannomutase-2 (PMM-2), thus hindering the conversion of mannose-6-phosphate to mannose-1-phosphate.[5] As a consequence, the synthesis of the sugar donor GDP-mannose decreases and, consequently, a general hypoglycosylation of many different glycoconjugates is found (Scheme 1).

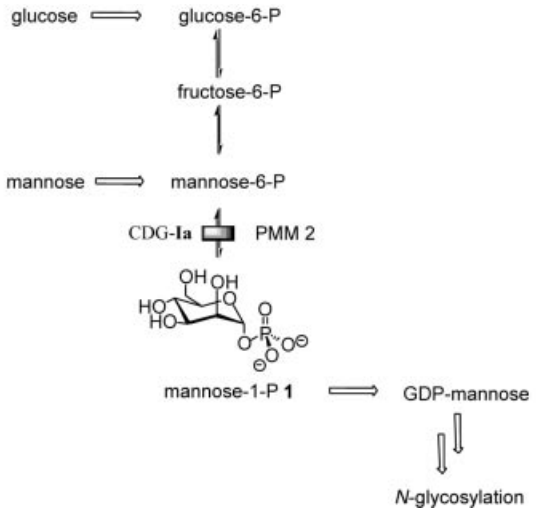

Scheme 1. Hexose metabolism into GDP-mannose and the CDG-**Ia** glycosylation defect

A therapeutic approach could be the intracellular delivery of mannose-1-phosphate (**1**, Scheme 1). This compound does not easily penetrate cellular membranes due to its high polarity and rapid dephosphorylation in the blood. The phosphate moiety offers a suitable site to attach degradable

[a] Institut für Organische Chemie, Universität Hamburg, Martin-Luther-King-Platz 6, 20146 Hamburg, Germany
[b] Klinik und Poliklinik für Kinderheilkunde, Albert-Schweitzer-Straße 33, 48129 Münster, Germany

lipophilic masking carrier residues. A suitable mannose-1-phosphate prodrug has to fulfil two requirements: (i) it has to be lipophilic enough for passive diffusion through the membrane, and (ii) it should be able to deliver mannose-1-phosphate hydrolytically and/or enzymatically, leaving a non-toxic group.[6] One elegant prodrug approach is the *cyclo*Sal strategy.[7] This approach has been developed in our laboratories and it is well established for the intracellular delivery of antiviral active nucleotide analogues like 2′,3′-dideoxy-2′,3′-didehydrothymidine monophosphate (d4TMP)[8] or 5-[(*E*)-bromovinyl]-2′-deoxyuridine monophosphate (BVdUMP).[9] The *cyclo*Sal approach is based upon a selective chemical hydrolysis mechanism. The chemically induced hydrolysis mechanism of the phosphate triester **2** involves a coupled cleavage of the phenyl ester leading to the benzyl diester **3**, which then leads to the phosphorylated drug **4** and salicyl alcohol **5** (Scheme 2), thus only one activation step is needed without a required enzymatic triggering.

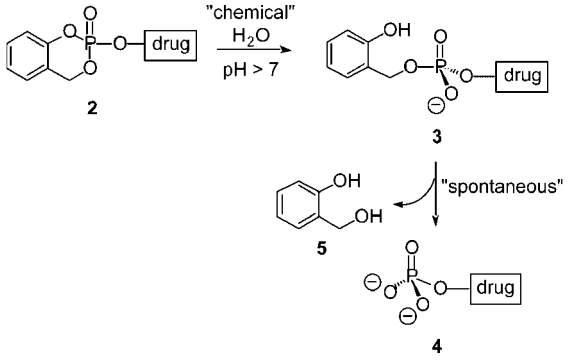

Scheme 2. Delivery mechanism of the *cyclo*Sal approach

A detailed description of the releasing mechanism has been reviewed recently.[7,10] The hydrolysis stability of the *cyclo*Sal phosphate triesters can be fine-tuned by the electronic properties of the substituents in the aromatic moiety. A reasonable half-life of the phosphate triester is a prerequisite for sufficient cellular uptake. One advantage of the *cyclo*Sal strategy as compared to other prodrug approaches for monophosphorylated compounds[11] is the favorable drug/masking group ratio of 1:1. This is a noteworthy aspect, because these substances have to be provided as dietary substitutes.

Here, we report on the synthesis of acetylated *cyclo*Sal-mannose-1-phosphates **6**−**9** and, for comparison, of *cyclo*-Sal-glucose-1-phosphates **10**, **11**. Furthermore, we report on insights into the hydrolysis mechanism of this new class of "carbohydrate prodrugs". These compounds were found to be able to deliver pyranose-1-phosphates. Finally, a complete correction of the CDG-**Ia** phenotype was observed in vitro in PMM-2-deficient fibroblasts proving the intracellular monophosphate delivery.

Results and Discussion

Chemical Synthesis

The convergent synthesis of *cyclo*Sal-pyranosyl-1-monophosphates **6**−**11** is shown in Scheme 3. D-Glucose (**12**) and D-mannose (**13**) were peracetylated to give compounds **14** and **15**, respectively, by treatment with acetic anhydride in pyridine as solvent in 96−98% yield.[12] The 1-*O*-acetyl groups were cleaved selectively using an equimolar amount of sodium methoxide at room temperature to give 2,3,4,6-tetra-*O*-acetyl-D-glucopyranose (**16**) and 2,3,4,6-tetra-*O*-acetyl-D-mannopyranose (**17**) in 72% and 58% yield, respectively.[13] The *cyclo*Sal moiety was prepared from differently substituted salicylic alcohols[14] **18**−**21** and phosphorus trichloride to yield cyclic chloridophosphites **22**−**25**. These compounds were isolated by distillation under nitrogen in 33−80% yield.[8] The *cyclo*Sal-pyranosyl-1-monophosphates **6**−**11** are obtained in a "one-pot reaction" by coupling the protected pyranoses **16**, **17** with the chloridophosphites **22**−**25** at −20 °C in the presence of diisopropylethylamine (DIPEA) in dry acetonitrile. Subsequent oxidation with *tert*-butyl hydroperoxide at ambient temperature gave the *cyclo*Sal-pyranosyl-1-monophosphates **6**−**11** in 6−62% yield. After chromatographic purification, *cyclo*Sal derivatives **6**−**11** were characterized by means of ^{1}H, ^{13}C and ^{31}P NMR spectroscopy as well as electrospray mass spectrometry. The mannose compounds **6**−**9**, as well as the glucose compounds **10**, **11**, were found to have only the α-configuration at the anomeric center. The α-glycosidic structure of *cyclo*Sal derivatives **10**, **11** was determined from the 1-H/2-H coupling constants ($^{3}J_{1,2} \approx 3.3-3.5$ Hz). ^{13}C-gated NMR spectroscopy was used to determine the anomeric configuration of the mannose derivatives **6**−**9**;[15,16] $^{1}J_{C\text{-}1,1\text{-}H}$ coupling constants of about 180 Hz again confirmed its α-glycosidic structure. Consequently, the phosphate triesters **6**−**11** display only two closely spaced signals in the ^{31}P NMR spectra (1:1 mixtures, $\delta = -9.0$ to -11.0 ppm), corresponding to the presence of two diastereomers resulting from mixed stereochemistry at the phosphorus center.

Hydrolysis Studies

^{31}P NMR experiments were carried out in mixtures of DMSO and imidazole/HCl buffer solutions at pH = 7.3. This technique allows a precise monitoring of the hydrolysis process, the intermediates and final products, as well as the determination of the product ratio. Further structural information on the hydrolysis products was obtained from proton-coupled ^{31}P NMR experiments. First, the ^{31}P NMR spectroscopic chemical shifts of the expected hydrolysis products 2,3,4,6-tetra-*O*-acetyl-D-mannose-1-phosphate (**26**) and *cyclo*saligenyl phosphate (**27**) were determined. Thus, dibenzyl 2,3,4,6-tetra-*O*-acetyl-D-mannopyranosyl-1-phosphate was prepared using the phosphoramidite/1*H*-tetrazole strategy. The *N*,*N*-diethylphosphoramidite used was obtained by treating dichloro(diethylamino)phosphane with 2 equiv. of benzyl alcohol in the presence of triethyl-

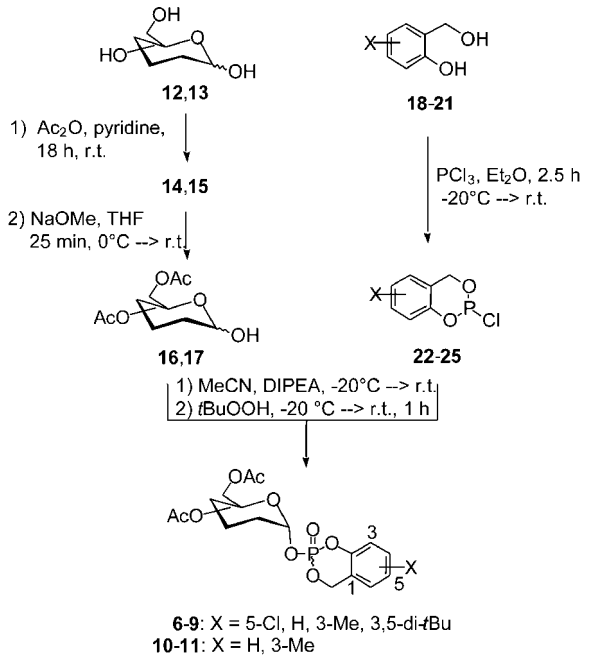

Scheme 3. Convergent synthesis strategy of *cyclo*Sal-pyranosyl-phosphate triesters **6**−**11**

amine.[17,18] The reference substance **26** was finally obtained by reductive debenzylation of dibenzyl 2,3,4,6-tetra-*O*-acetyl-D-mannopyransyl-1-phosphate. The ^{1}H-^{31}P NMR COSY spectrum of **26**, measured in a TRIS buffer/DMSO solution, shows a cross-peak of 1-H (δ = 5.25 ppm) with the phosphorus resonance signal (δ = 0.5 ppm). The resonance signal of 1-H shows the expected spin couplings with 2-H ($^{3}J_{1,2}$ = 1.2 Hz) and with the phosphorus atom ($^{2}J_{1,P}$ = 7.6 Hz). The proton-coupled ^{31}P NMR spectrum likewise shows a resonance signal with doublet splitting at δ = 0.5 ppm and a coupling constant of $^{3}J_{1,P}$ = 7.6 Hz. *cyclo*Saligenyl phosphate diester **27**, the expected product of a cleavage of the glycosidic bond, was synthesized from *cyclo*saligenyl chloridophosphite (**23**) by oxidation with *tert*-butyl hydroperoxide in water. In the ^{31}P NMR spectrum in [D_6]DMSO, a signal was observed at δ = −7.6 ppm with a triplet splitting caused by the two benzylic protons.

The hydrolysis of the *cyclo*Sal triester **7** in 25 mM imidazole/HCl buffer at pH = 7.3 clearly shows the two resonances of the (R_P/S_P)-configured triester (δ = −9.8 and −9.4 ppm) as well as a triplet at δ = −6.0 ppm resulting from the *cyclo*saligenyl phosphate diester **27**. The difference of the chemical shifts of **27** (Δδ = 1.6 ppm) in both experiments is caused by the use of different solvent systems. In comparison, compound **26** also shows the same shift of the resonance signal when changing the solvents. Nevertheless, the coupling constants remain unchanged. Additionally, a ddd system (virtual quadruplet) appears at δ = −1.2 ppm (Figure 1). This signal decreases with time and a doublet appears at δ = −0.9 ppm. The dependence of these two peaks points to the formation of 2,3,4,6-tetra-*O*-acetyl-D-mannose-1-phosphate (**26**) from the intermediate showing the resonance signal at δ = −1.2 ppm. Assuming that the hydrolysis proceeds as in the case of the nucleotide delivery systems[7], this points to the cleavage of the phenyl ester bond of the triester **7** leading to a benzyl phosphate diester

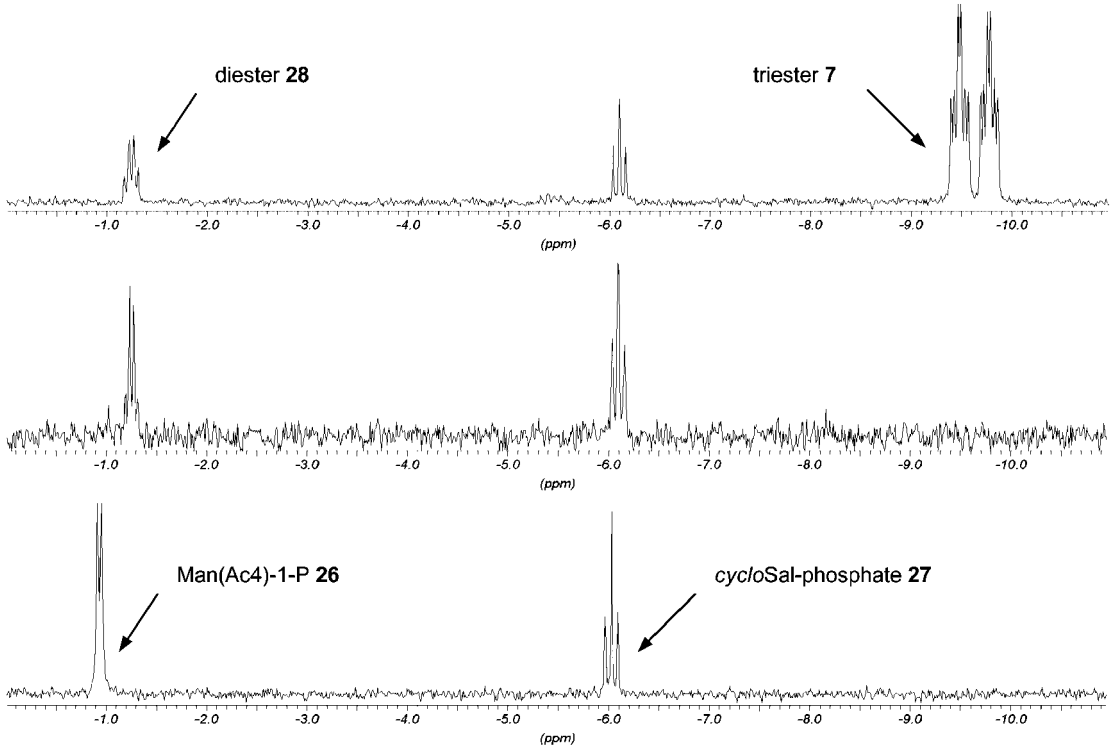

Figure 1 ^{1}H-coupled ^{31}P NMR hydrolysis study of *cyclo*Sal-2,3,4,6-tetra-*O*-acetyl-α-D-mannopyranosyl-1-phosphate (**7**)

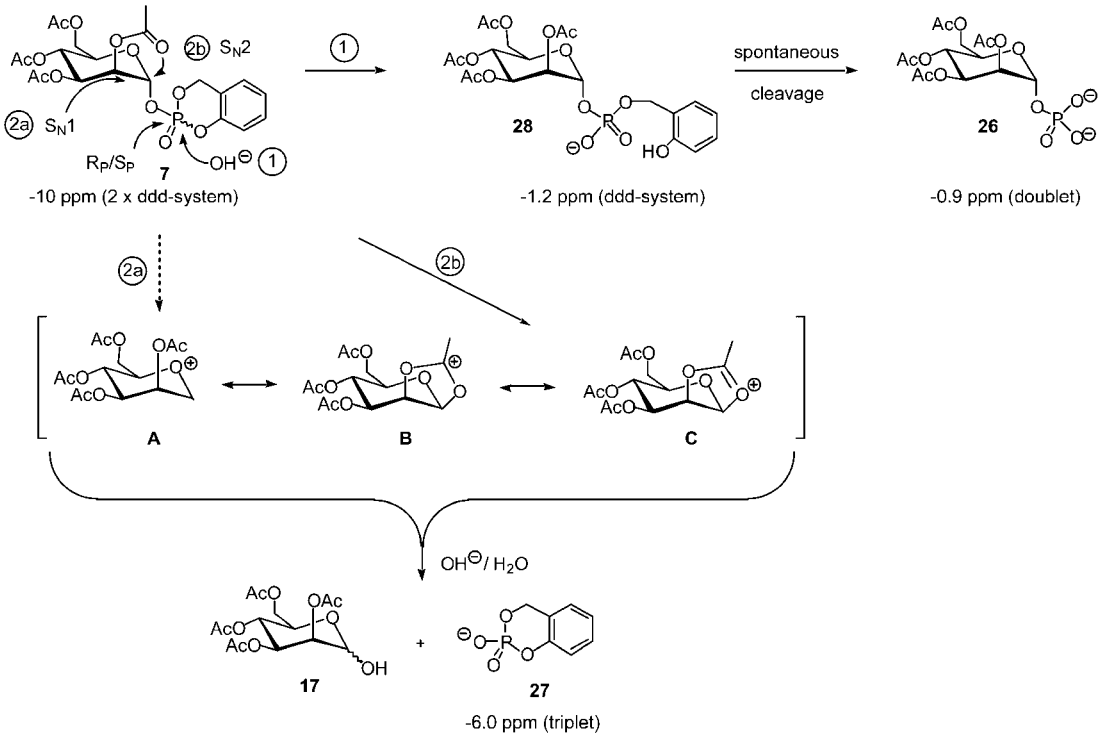

Scheme 4. Hydrolysis mechanism for *cyclo*Sal-mannose-1-phosphates **6**−**9**

(such as **28** in Scheme 4). The diastereotopic protons of the benzylic methylene group and the anomeric 1-H lead to the ddd splitting pattern. Thus, the formation of a benzyl diester of type **28** as a hydrolysis intermediate is confirmed by the chemical shift and the coupling structure (Figure 1).

The *cyclo*Sal-pyranosyl-1-phosphates **6**−**11** were hydrolyzed in 25 mM phosphate buffer at pH = 7.3 to estimate their chemical stability. For comparison, the epimeric glucose analogues **10**, **11** were included. The hydrolysis pathways are shown in Scheme 4 and results are summarized in Tables 1 and 2. The determined half-lives for both pyranose compound series were unexpectedly considerably shorter ($t_{1/2}$ = 0.07−0.18 h and 1.19−1.42 h, respectively) than the values found for the *cyclo*Sal nucleotides[7]. There, the 3-methyl substituent in the *cyclo*Sal moiety led to half-lives of the corresponding phosphate triesters of 8−16 h. Furthermore, two clear effects related to the electronic properties of the substituents of the salicylic alcohol were observed: (1) the stronger the electron-withdrawing effect of the substituent, the shorter the hydrolysis half-life. This result strongly correlates with the data found for *cyclo*Sal nucleotides using the same hydrolysis conditions, and (2) the longer the hydrolysis half-lives, the lower the amount of 2,3,4,6-tetra-*O*-acetyl-D-mannose-1-phosphate (**26**) formed (Table 1).

These results and the NMR couplings shown in Figure 1 led to an analogous hydrolysis mechanism based on the *cyclo*Sal concept (Scheme 4). The *cyclo*Sal-mannose-1-monophosphates **6**−**9** were hydrolyzed by two concurrent hydrolysis pathways. (1) A nucleophilic attack of hydroxide or water at the phosphate group leads to the formation of the benzyl phosphate diester **28** (ddd system) as a virtual quadruplet at δ = −1.2 ppm and the loss of the stereogenic P-center. This selective cleavage of the phenyl ester bond converts the *ortho* substituent of the benzyl group from a very weak donor (phosphate) to a strong donor group (hydroxy). Next, the benzyl phosphate diester **28** decomposes spontaneously to acetylated mannose-1-phosphate **26** with an NMR resonance at δ = −0.9 ppm and a doublet splitting (pathway 1). (2) In addition, the glycosidic bond is

Table 1. Half-lives and product distribution of the mannose-1-phosphate triesters **6**−**9**

Mannose-1-phosphate triesters **6**−**9**	$t_{1/2}$ [h]	Product distribution [%]	
		Acetylated mannose-1-phosphate **26**	Acetylated mannose **17**
5-Cl-*cyclo*Sal-($ManAc_4$)-1-phosphate (**6**)	0.07	70	30
*cyclo*Sal-($ManAc_4$)-1-phosphate (**7**)	0.12	64	36
3-Me-*cyclo*Sal-($ManAc_4$)-1-phosphate (**8**)	0.18	52	48
3,5-Di-*t*Bu-*cyclo*Sal-($ManAc_4$)-1-phosphate (**9**)	−[a]	37	63

[a] Insoluble under experimental conditions.

Table 2. Distribution of the hydrolysis products and half-lives of the pyranosyl phosphate triesters **7**, **8**, **10**, **11**

Pyranose-1-phosphate triesters **7**,**8**,**10**,**11**	$t_{1/2}$ [h]	Product distribution [%]	
		Acetylated pyranosyl-1-phosphate	Acetylated sugar
*cyclo*Sal-($ManAc_4$)-1-phosphate (**7**)	0.12	64	36
3-Me-*cyclo*Sal-($ManAc_4$)-1-phosphate (**8**)	0.18	52	48
*cyclo*Sal-($GlucAc_4$)-1-phosphate (**10**)	1.19	92	8
3-Me-*cyclo*Sal-($GlucAc_4$)-1-phosphate (**11**)	1.42	90	10

cleaved by an S_N1-type reaction. The resulting stabilized oxocarbenium ion **A** forms 2,3,4,6-tetra-*O*-acetyl-D-mannopyranose **17** after quenching. The concomitant product is *cyclo*saligenyl phosphate **27**. Its benzylic protons cause the triplet splitting pattern at $\delta = -6.0$ ppm. This cyclic phosphate diester **27** is not hydrolyzed further due to the negative charge at the phosphorus atom (pathway 2). The importance of pathway 1 is dependent on the substituents in the aromatic ring while the cleavage of the glycosidic bond should be a constantly proceeding reaction. Consequently, the faster the hydrolysis by pathway 1 proceeds, the more of the monophosphate is obtained. The product distribution found in the hydrolyses supports this interpretation (Table 1).

Furthermore, a comparison was made between the epimeric *gluco* and *manno* derivatives. Most striking was the 10-fold increase of the hydrolysis half lives from minutes to hours (Table 2). In addition, the *gluco* compounds **10**, **11** deliver considerably higher amounts of acetylated pyranosyl-1-monophosphate than the *manno* compounds **6**−**9**.

Obviously, an anchimeric acceleration leading to an acetoxonium ion **B**, **C** (pathway 2b, Scheme 4) takes place for the *manno* derivatives **6**−**9** in addition to the S_N1-type cleavage, leading to the formation of the oxocarbenium ion **A** (pathway 2a, Scheme 4). Nevertheless, although the cleavage reaction was found to be not as selective as in the case of the *cyclo*Sal nucleotides, the mannose derivatives **6**−**9**

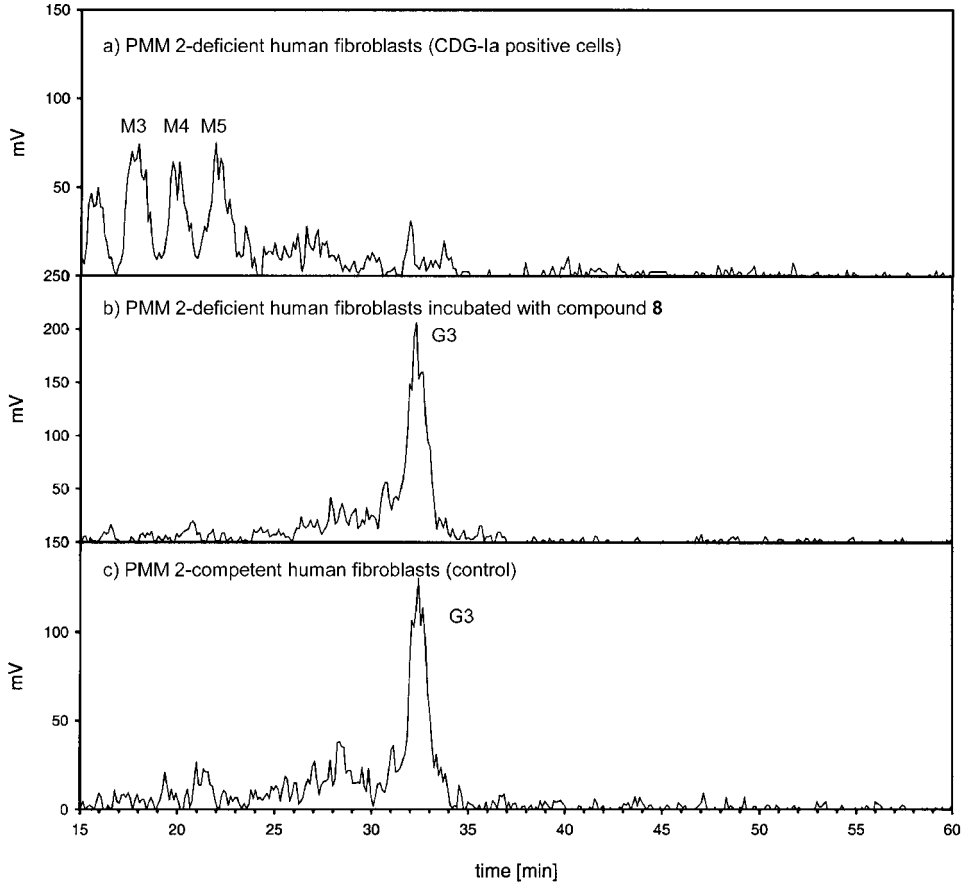

Figure 2. HPLC chromatogram of the LLO analysis of compound **8** (G3 = $Glc_3Man_9GlcNAc_2$; M3 = $Man_3GlcNAc_2$; M4 = $Man_4GlcNAc_2$; M5 = $Man_5GlcNAc_2$)

release considerable amounts of mannose-1-phosphate from the lipophilic precursor.

Biological Tests

Finally, the biological activity of the *cyclo*Sal-mannose-1-phosphates **6**−**9** was tested in vitro in fibroblasts. Healthy fibroblasts assemble complete oligosaccharide chains having a $Glc_3Man_9GlcNAc_2$ structure (G3; Figure 2, c). In contrast, PMM-2-deficient fibroblasts synthesize only truncated oligosaccharide chains with $Man_4GlcNAc_2$ (M4) and $Man_3GlcNAc_2$ structures (M3; Figure 2, a). A successful delivery of mannose-1-phosphate (**1**) from a lipophilic precursor should lead to complete correction of this glycosylation pattern. Thus, the G3 structure should be observed. Triesters **6**, **7**, **9** did not cause this correction. However, 3-Me-*cyclo*Sal-tetra-*O*-acetyl-α-D-mannose-1-phosphate (**8**) showed a total correction of the hypoglycosylation pattern (Figure 2, b). In this case, the efficient intracellular delivery of mannose-1-phosphate can be concluded. Moreover, the observed bioactivity also proves that the acetyl groups attached to the glycon are cleaved intracellularly by (carboxy)esterases. Obviously, triester **8** has the correct combination of properties to act as a Man-1-MP prodrug. This result offers, in principle, a way to use such compounds as therapeutics.

Conclusion

The presented data clearly indicate that the *cyclo*Sal approach originally developed for the delivery of antivirally active nucleotides can be transferred to the delivery of pyranose-1-phosphates. However, oxocarbenium ion formation and the anchimeric effect reduce the selectivity of the delivery mechanism. Nevertheless, the comparison with the glucose derivatives clearly proves that the delivery mechanism is strongly influenced by the attached hexose. Further experiments to verify this using 2-deoxy and 2-fluoro derivatives are currently under way in our laboratories. Finally, as for the nucleotides, the promising total correction of the hypoglycosylation found in the biological assays shows that the delivery of biologically active phosphorylated compounds from *cyclo*Sal phosphate triesters may lead to a strong improvement in the bioactivity.

Experimental Section

Synthesis: NMR spectra were recorded with a Bruker AC 250-P, Bruker AMX 400 and Bruker DRX 500 Fourier transform spectrometers. All ^1H and ^{13}C NMR chemical shifts (δ) are quoted in ppm and calibrated with respect to the residual protonated solvent signals. The ^{31}P NMR chemical shifts are quoted in ppm using H_3PO_4 as the external reference. Coupling constants (*J*) are given in Hz. The spectra were recorded at room temperature. Electron impact mass spectra were measured with a VG Analytical VG/70−250S spectrometer (double focussing). Merck precoated 60 F_{254} plates with a 0.2 mm layer of silica gel were used for thin-layer chromatography (TLC). Detection was effected by observation under UV light at 254 nm, or by spraying with 10% ethanolic sulfuric acid and subsequent heating. All preparative TLCs were performed with a chromatotron (Harrison Research, Model 7924T) using glass plates coated with 1 mm or 2 mm layers of Merck 60 PF_{254} silica gel containing a fluorescent indicator. Analytical HPLC was done with a Merck-Hitachi HPLC system (D-7000) equipped with a LiChroCART 125-3 column containing reversed-phase silica gel Lichrospher 100 RP 18 (5 μm). The lyophilized products **6**−**11** were found to be pure by rigorous HPLC analysis. All reactions were carried out under dry nitrogen except for the synthesis of **14**−**17**. Solvents used were commercially available dry solvents and were stored under argon in the presence of molecular sieves (Fluka). Acetonitrile was dried with sodium/benzophenone and distilled under nitrogen. The diastereomeric ratios of the phosphate triesters were determined by integration of the ^{31}P NMR spectra.

General Procedure for the Preparation of *cyclo*Sal-pyranose-1-phosphates 6−11: The acetylated monosaccharides **16** or **17** (1.0 equiv.) and DIPEA (2.0−2.5 equiv.) were dissolved in MeCN (ca. 0.025 M) at −20 °C under an inert gas. The corresponding saligenyl chloridophosphite **22**−**25** (2.0−2.5 equiv.) was then added to this solution. The solutions were stirred at room temperature for 1.5 h for completion of the reaction (TLC analysis: CH_2Cl_2/MeOH, 9:1). The oxidation of the intermediate cyclic phosphite triester was achieved by addition of 3−4 equiv. of *tert*-butyl hydroperoxide (5−6 M solution in *n*-decane) at −20 °C. After the mixture was stirred (1 h) and warmed to room temperature, the solvent was removed under reduced pressure. The residues were purified twice by chromatography on silica gel plates of a chromatotron first using ethyl acetate/methanol (9:1) as solvent, followed by a gradient of dichloromethane in methanol, to yield the title compounds **6**−**11**.

Tetra-*O*-acetyl-(5-chloro-*cyclo*saligenyl)-α-D-mannopyranosyl-1-phosphate (6): Quantities: 2,3,4,6-Tetra-*O*-acetyl-α-D-mannopyranose (**17**, 200 mg, 0.57 mmol, 1.0 equiv.), DIPEA (153 μL, 1.15 mmol, 2.0 equiv.) dissolved in 5 mL of absolute MeCN, 5-chloro-*cyclo*saligenyl chloridophosphite (**22**, 256 mg, 1.15 mmol, 2.0 equiv.), 690 μL of *t*BuOOH. After chromatography, the triester **6** was isolated as a slightly yellow foam; yield 19.5 mg (0.03 mmol, 6%), diastereomeric ratio 1.0:1.0, R_f = 0.75 (CH_2Cl_2/MeOH, 30:1), $[\alpha]_D^{20}$ = +0.28 (*c* = 0.7, $CHCl_3$). ^1H NMR (500 MHz, $CDCl_3$): δ = 1.96, 1.97, 1.99, 2.02, 2.07, 2.08, 2.13, 2.15, (s, 8 × 3 H), 3.96 (ddd, *J* = 5.7 Hz, 2.5 Hz, 1 H, 9.8 Hz), 3.97 (ddd, *J* = 9.5 Hz, 4.4 Hz, 1.9 Hz, 1 H), 4.16−4.06 (m, 3 H), 4.24 (dd, *J* = 12.6 Hz, 5.7 Hz, 2.5 Hz, 12.6 Hz, 2 H), 5.42−5.16 (m, 10 H), 5.63 (dd, *J* = 1.9, *J* = 6.2 Hz, 1 H), 5.74 (dd, *J* = 1.9 Hz, 6.3 Hz, 1 H), 6.99−7.06, 7.09−7.16, 7.29−7.33 (m, 6 H) ppm. ^{13}C NMR (100 MHz, $CDCl_3$): δ = 20.95, 21.09, 21.11, 21.17, 21.22, 21.28, 21.30, 62.07, 62.36, 65.58, 65.94, 68.56, 68.70, 68.98, 69.11, 69.22, 69.74 (d, *J* = 4.6 Hz), 70.83, 71.07, 96.34, 96.40 (d, *J* = 5.3 Hz), 115.05, 123.38, 123.42, 124.72, 124.75, 126.68, 126.75 (d, *J* = 9.3 Hz), 131.86, 131.88, 148.45, 148.73 (d, *J* = 7.3 Hz), 171.53, 171.89, 172.12 ppm. ^{31}P NMR (202 MHz, $CDCl_3$): δ = −11.0, −11.2 ppm. MS (ESI^+): *m*/*z* = 573.3 [M + Na^+], 589.3 [M + K^+].

Tetra-*O*-acetyl-*cyclo*saligenyl-α-D-mannopyranosyl-1-phosphate (7): Quantities: 2,3,4,6-Tetra-*O*-acetyl-α-D-mannopyranose (**17**, 150 mg, 0.43 mmol, 1.0 equiv.), DIPEA (183 μL, 1.07 mmol, 2.5 equiv.) dissolved in 5 mL of absolute MeCN, *cyclo*saligenyl chloridophosphite (**23**, 203 mg, 1.07 mmol, 2.5 equiv.), 140 μL of *t*BuOOH. After chromatography, triester **7** was isolated as a colorless foam; yield 131.3 mg (0.25 mmol, 59%), diastereomeric ratio 1.0:1.0, R_f = 0.71 (CH_2Cl_2/MeOH, 30:1), $[\alpha]_D^{20}$ = +0.06 (*c* = 0.17, $CHCl_3$). ^1H NMR (500 MHz, $CDCl_3$): δ = 1.94, 1.95, 1.97, 2.00, 2.07, 2.08, 2.12, 2.13 (s, 8 × 3 H), 3.96 (ddd, *J* = 9.7 Hz, 5.2 Hz, 2.9 Hz, 1 H), 4.03 (dd, *J* = 12.2 Hz, 2.5 Hz, 1 H), 4.09 (dd, *J* =

12.5 Hz, 2.9 Hz, 1 H), 4.15 (ddd, J = 9.7 Hz, 5.0 Hz, 2.5 Hz, 1 H), 4.24 (dd, J = 12.5 Hz, 12.2 Hz, 5.2 Hz, 5.0 Hz, 2 H), 5.22 (dd, J = 3.1 Hz, 1.9 Hz, 1 H), 5.25−5.43 (m, 9 H), 5.73 (dd, J = 1.9 Hz, 6.7 Hz, 1 H), 5.80 (dd, J = 1.9 Hz, 6.2 Hz, 1 H), 7.04−7.18 (m, 6 H), 7.30−7.35 (m, 2 H). ^{13}C NMR (101 MHz, $CDCl_3$): δ = 20.93, 20.95, 20.97, 20.99, 21.08, 21.11, 62.17, 62.29, 65.55, 65.77, 68.31, 68.49, 68.60, 68.95, 68.98, 69.08, (d, J = 4.4 Hz), 70.95, 71.02 (C-5), 96.30, 96.44 (d, J = 5.4 Hz), 115.83, 115.88, 119.08, 119.28 (d, J = 9.3 Hz), 120.91, 121.09, 125.85, 126.06, 130.56, 131.01, 150.19, 150.26 (d, J = 7.0 Hz), 169.83 169.89, 169.93, 170.10, 170.53, 170.96, 171.00 ppm. ^{31}P NMR (202 MHz, $CDCl_3$): δ = −10.7, −10.8 ppm. MS (ESI^+): m/z = 539.3 [M + Na^+], 555.3 [M + K^+].

Tetra-*O*-acetyl-(3-methyl-*cyclo*saligenyl)-α-D-mannopyranosyl-1-phosphate (8): Quantities: 2,3,4,6-Tetra-*O*-acetyl-α-D-mannopyranose (**17**, 99 mg, 0.28 mmol, 1.0 equiv.), DIPEA (121 μL, 0.71 mmol, 2.5 equiv.) dissolved in 4 mL of absolute MeCN, 3-methyl-*cyclo*saligenyl chloridophosphite (**24**, 144 mg, 0.71 mmol, 2.5 equiv.), 140 μL of *t*BuOOH. After chromatography, the triester **8** was isolated as a colorless foam; yield 62.0 mg (0.12 mmol, 62%), diastereomeric ratio 1.0:1.0, R_f = 0.89 (CH_2Cl_2/MeOH, 30:1), $[\alpha]_D^{20}$ = +0.03 (c = 0.35, $CHCl_3$). ^{1}H NMR (500 MHz, $CDCl_3$): δ = 1.96, 1.99, 2.01, 2.02, 2.03, 2.07, 2.09, 2.11, 2.30, 2.31, (s, 10 × 3 H), 3.96 (ddd, J = 10.1 Hz, 5.7 Hz, 2.5 Hz, 1 H), 4.02 (dd, J = 2.5 Hz, 12.6 Hz, 1 H), 4.14 (dd, J = 5.7 Hz, 12.6 Hz, 1 H), 4.19 (ddd, J = 9.5 Hz, 5.0 Hz, 1.9 Hz, 1 H), 4.30 (dd, J = 11.9 Hz, 5.0 Hz, 1.9 Hz, 11.9 Hz, 2 H), 5.42−5.29 (m, 10 H), 5.96 (dd, J = 1.2 Hz, 6.9 Hz, 1 H), 6.04 (dd, J = 1.9 Hz, 6.3 Hz, 1 H), 6.93−6.98, 7.04−7.09, 7.19−7.22 (m, 6 H). ^{13}C NMR (101 MHz, $CDCl_3$): δ = 15.75, 20.05, 20.95, 21.09, 21.11, 21.17, 21.22, 21.28, 21.30, 62.04, 62.35, 65.53, 65.83, 68.53, 68.58, 68.58, 68.62, 67.36, 69.45 (d, J = 4.6 Hz), 70.02, 71.08, 96.22, 96.35 (d, J = 5.5 Hz), 115.03, 115.05, 123.38, 123.42, 124.72, 124.75, 126.68, 126.75 (d, J = 9.3 Hz), 131.86, 131.88, 155.45, 155.73 (d, J = 7.3 Hz), 169.35, 169.53, 169.60 ppm. ^{31}P NMR (202 MHz, $CDCl_3$): δ = −9.9, −10.2 ppm. MS (ESI^+): m/z = 553.4 [M + Na^+], 569.3 [M + K^+].

Tetra-*O*-acetyl-(3,5-di-*tert*-butyl-*cyclo*saligenyl)-α-D-mannopyranosyl-1-phosphate (9): Quantities: 2,3,4,6-Tetra-*O*-acetyl-α-D-mannopyranose (**17**, 150 mg, 0.43 mmol, 1.0 equiv.), DIPEA (151 μL, 0.86 mmol, 2.0 equiv.) dissolved in 6 mL of absolute MeCN, 3,5-di-*tert*-butyl-*cyclo*saligenyl chloridophosphite (**25**, 259 mg, 0.86 mmol, 2.0 equiv.), 192 μL of *t*BuOOH. After chromatography, the triester **9** was isolated as a colorless foam; yield 160 mg (0.26 mmol, 61%), diastereomeric ratio 1.0:0.7, R_f = 0.57 (CH_2Cl_2/MeOH, 30:1), $[\alpha]_D^{20}$ = +0.25 (c = 0.55, $CHCl_3$). ^{1}H NMR (500 MHz, $CDCl_3$): δ = 1.30, 1.31, 1.42 (s, 36 H), 1.97, 1.99, 2.02, 2.03, 2.08, 2.09, 2.16, 2.17 (s, 8 × 3 H), 4.08−4.17 (m, 4 H), 4.24−4.32 (m, 2 H), 5.24−5.40 (m, 10 H), 5.82 (dd, J = 1.8 Hz, 6.4 Hz, 1 H), 5.85 (dd, J = 1.8 Hz, 6.9 Hz, 1 H), 6.95−7.00, 7.35−7.37, (m, 4 H) ppm. ^{13}C NMR (101 MHz, $CDCl_3$): δ = 21.01, 21.07, 21.10, 20.21, 20.95, 25.37, 30.28, 31.79, 35.67, 62.04, 62.35, 65.53, 65.83, 68.53, 68.58, 68.58, 68.62, 69.36, 69.45 (d, J = 4.6 Hz), 70.02, 71.08, 96.34, 96.40 (d, J = 5.2 Hz), 120.90, 121.00, 125.22, 125.35, 126.95, 126.98, 134.69, 133.72, 140.49, 149.68, 149.79 (d, J = 7.1 Hz), 170.28, 170.34, 170.49, 170.52. ^{13}C-gated (101 MHz, $CDCl_3$): δ [ppm] = 96.4 (d, J = 178.0 Hz) ppm. ^{31}P NMR (202 MHz, $CDCl_3$): δ [ppm] = −9.2, −9.7 ppm. MS (ESI^+): m/z = 651.4 [M + Na^+], 667.4 [M + K^+].

Tetra-*O*-acetyl-*cyclo*saligenyl-α-D-glucopyranosyl-1-phosphate (10): Quantities: 2,3,4,6-Tetra-*O*-acetyl-D-glucopyranose (**16**, 150 mg, 0.43 mmol, 1.0 equiv.), DIPEA (151 μL, 0.86 mmol, 2.0 equiv.) dissolved in 6 mL of absolute MeCN, *cyclo*saligenyl chloridophosphite (**23**, 162 mg, 0.86 mmol, 2.0 equiv.), 270 μL of *t*BuOOH. After chromatography, triester **10** was isolated as a colorless foam; yield 51 mg (0.10 mmol, 23%), diastereomeric ratio 1.0:0.7, R_f = 0.68 (CH_2Cl_2/MeOH, 30:1), $[\alpha]_D^{20}$ = +0.03 (c = 0.25, $CHCl_3$). ^{1}H NMR (500 MHz, $CDCl_3$): δ = 1.97, 1.99, 2.01, 2.02, 2.03, 2.08, 2.09, 2.11 (s, 8 × 3 H, CH_3), 3.98−4.01 (m, 2 H), 4.09−4.14 (m, 2 H), 4.20−4.30 (m, 2 H), 4.99 (dd, J = 2.7 Hz, 3.3 Hz, 1 H), 5.04 (dd, J = 2.7 Hz, 3.5 Hz, 1 H), 5.12 (dd, J = 9.6 Hz, 9.7 Hz, 9.6 Hz, 9.7 Hz, 2 H), 5.36−5.49 (m, 6 H), 5.97 (dd, J = 3.3 Hz, 6.6 Hz, 1 H), 6.04 (dd, J = 3.5 Hz, 6.9 Hz, 1 H), 7.06−7.22 (m, 6 H), 7.34−7.40 (m, 2 H) ppm. ^{13}C NMR (101 MHz, $CDCl_3$): δ = 20.75, 20.90, 21.02, 21.05, 62.38, 62.47, 67.21, 67.25, 68.53, 68.62 (d, J = 6.1 Hz), 68.97, 69.02, 70.13, 70.28, 71.26, 71.32, 96.81, 96.89 (d, J = 5.0 Hz), 115.83, 115.88, 119.24, 119.31, 120.97, 121.12, 126.01, 126.08 (d, $^3J_{C1,P}$ = 9.0 Hz, C-1 aryl), 131.04, 131.11, 151.57, 151.79 (d, J = 7.0 Hz), 169.66, 169.82, 170.13, 170.52, 170.94 ppm. ^{31}P NMR (202 MHz, $CDCl_3$): δ = −10.3, −10.6 ppm. MS (ESI^+): m/z = 539.3 [M + Na^+], 555.3 [M + K^+].

Tetra-*O*-acetyl-(3-methyl-*cyclo*saligenyl)-α-D-glucopyranosyl-1-phosphate (11): Quantities: 2,3,4,6-Tetra-*O*-acetyl-D-glucopyranose **16** (150 mg, 0.43 mmol, 1.0 equiv.), DIPEA (150 μL, 0.88 mmol, 2.0 equiv.) dissolved in 6 mL of absolute MeCN, 3-methyl-*cyclo*saligenyl chloridophosphite (**24**, 185 mg, 0.91 mmol, 2.1 equiv.), 270 μL of *t*BuOOH. After chromatography, the triester **11** was isolated as a colorless foam; yield 87 mg (0.16 mmol, 38%), diastereomeric ratio 1.0:1.0, R_f = 0.66 (CH_2Cl_2/MeOH, 30:1), $[\alpha]_D^{20}$ = +0.45 (c = 0.37, $CHCl_3$). ^{1}H NMR (500 MHz, $CDCl_3$): δ = 2.11, 2.09, 2.07, 2.03, 2.02, 2.01, 1.99, 1.96 (s, 8 × 3 H), 2.31, 2.30 (s, 2 × 3 H), 3.96−4.04 (m, 2 H), 4.14 (dd, J = 5.0 Hz, 11.9 Hz, 1 H), 4.19 (ddd, J = 2.5 Hz, 4.4 Hz, 10.0 Hz, 1 H), 4.25 (dd, J = 2.3 Hz, 11.9 Hz, 1 H), 4.27 (dd, J = 4.4, J = 12.0 Hz, 1 H), 4.98 (dd, J = 10.2 Hz, 3.3 Hz, 1 H), 5.03 (dd, J = 10.2 Hz, 3.3 Hz, 1 H), 5.12 (dd, J = 9.9 Hz, 9.9 Hz, 9.5 Hz, 10.0 Hz, 2 H), 5.32−5.48 (m, 6 H), 5.97 (dd, J = 3.3 Hz, 6.6 Hz, 1 H), 6.05 (dd, J = 3.3 Hz, 7.1 Hz, 1 H), 6.94−6.98, 7.19−7.23, 7.04−7.10 (m, 6 H) ppm. ^{13}C NMR (101 MHz, $CDCl_3$): δ = 15.70, 15.76, 20.70, 20.81, 20.92, 21.03, 21.07, 61.35, 61.69, 67.83, 67.85, 67.36, 67.43 (d, $^2J_{C7,P}$ = 4.6 Hz), 68.82, 68.89, 69.39, 69.63, 70.06, 70.21 (d, J = 7.0 Hz), 95.01, 95.06 (d, J = 6.1 Hz), 117.60, 117.64, 123.59, 123.63, 124.68, 124.73, 126.68, 126.75 (d, J = 9.3 Hz), 132.28, 132.21, 148.53, 148.69 (d, J = 7.3 Hz), 169.67, 169.77, 171.23 ppm. ^{31}P NMR (202 MHz, $CDCl_3$): δ = −9.5, −9.7 ppm. MS (ESI^+): m/z = 553.4 [M + Na^+], 569.4 [M + K^+].

Biological Tests: To determine the correct assembly of lipid-linked oligosaccharides (LLO) primary dermal fibroblasts of CDG-**Ia** patients were incubated in a medium containing [2-^{3}H]mannose. Full length LLO contains two *N*-acetylglucosaminyl, nine mannosyl and three glucosyl residues and was labeled with [2-^{3}H]-mannose. After the incubation, radioactively labeled oligosaccharides were extracted and the carbohydrate portion was analysed by HPLC. Substances were dissolved in the labelling medium to study their influence on oligosaccharide biosynthesis of the disease cells (PMM2-deficient). These cells predominantly synthesize truncated structures.[19]

Labeling of Human Fibroblasts: Fibroblasts were labeled for 2 h with 100 μCi [2-^{3}H]mannose (specific activity 10−20 Ci/mmol) per mL labeling medium (DMEM w/o glucose/MEM, 9:1), and washed with PBS. Each substance was dissolved in DMSO and added in 1 mM final concentration to the medium prior to labeling.

Extraction of LLO and PDO: For HPLC analysis, cells were extracted three times with chloroform/methanol (2:1). The pellet was dried under nitrogen and extracted several times with water. Dol-

ichylpyrophosphate-linked oligosaccharides were predominantly recovered from the subsequent chloroform/methanol/water (10:10:3) extract and released by mild acid hydrolysis in *n*-propanol/0.1 N HCl (1:2) at 100 °C for 20 min. HPLC was done in an acetonitrile/water gradient using a Microsorb MV column (Varian GmbH, Darmstadt, Germany) with a Waters Alliance system (Waters GmbH, Eschborn, Germany). The gradient started with acetonitrile/water (65:35) and changed to acetonitrile/water (35:65) during the run. A constant solvent flow of 0.5 mL/min was used.

Acknowledgments

Financial support by the Deutsche Forschungsgemeinschaft, Germany and the Fonds der Chemischen Industrie, Germany and the BMBF, Germany is gratefully acknowledged.

[1] T. Marquardt, H. Freeze, *Biol. Chem.* **2001**, *382*, 161−177.
[2] J. Jaeken, M. Vanderschueren-Lodeweyckx, P. Casaer, L. Snoeck, L. Coerbeel, E. Eggermont, R. Edckels, *Pediatr. Res.* **1980**, *14*, 179.
[3] H. Carchon, E. van Schaftingen, G. Matthijs, J. Jaeken, *Biochim. Biophys. Acta* **1999**, *1455*, 155−165.
[4] G. Matthijs, E. Schollen, E. van Schaftingen, J.-J. Cassiman, J. Jaeken, *Am. J. Hum. Genet.* **1998**, *62*, 542−550.
[5] G. Matthijs, E. Schollen, L. Heykanta, S. Grünewald, *Mol. Genet. Metab.* **1999**, *68*, 220−226.
[6] Only one further potential prodrug for phosphorylated pyranoses has been published. However, no delivery studies and no biological data were given: S. Rutschow, J. Thiem, C. Kranz, T. Marquardt, *Bioorg. Med. Chem.* **2002**, *10*, 4043−4049.
[7] C. Meier, *Mini-Rev. Med. Chem.* **2002**, *2*, 219−234.
[8] C. Meier, M. Lorey, E. De Clercq, J. Balzarini, *J. Med. Chem.* **1998**, *41*, 1417−1427.
[9] C. Meier, A. Lomp, A. Meerbach, P. Wutzler, *J. Med. Chem.* **2002**, *45*, 5157−5172.
[10] C. Meier, *Mini-Rev. Med. Chem.*, in press.
[11] C. Meier, *Synlett* **1998**, 233−242.
[12] J. Coniche, G. A. Levy, *Methods Carbohydr. Res.* **1963**, *2*, 345−347.
[13] T. Itoh, H. Takamura, K. Watanabe, Y. Akari, Y. Ishido, *Carbohydr. Res.* **1986**, *156*, 241− 246.
[14] C. Meier, E. De Clercq, J. Balzarini, *Eur. J. Org. Chem.* **1998**, 1837−1847.
[15] K. Bock, I. Lundt, C. Pedersen, *Tetrahedron Lett.* **1973**, *13*, 1037−1040.
[16] K. Bock, C. Pedersen, *J. Chem. Soc., Perkin Trans. 2* **1974**, 293−296.
[17] A. D. Briggs, M. Camplo, S. Freeman, J. Lundström, B. G. Pring, *Tetrahedron* **1996**, *47*, 14937−14950.
[18] G. Baisch, R. Öhrlein, *Bioorg. Med. Chem.* **1997**, *5*, 383−391.
[19] K. Panneerselvan, H. Freeze, *J. Clin. Invest.* **1996**, *97*, 1478−1487.

Received October 27, 2003

